Influence of partial substitution for carbon black with graphene oxide on dynamic properties of natural rubber composites

Huan Zhang[1], *Yintao Wei*[1] ✉, *Zhenran Kang*[1], *Guizhe Zhao*[2], *Yaqing Liu*[2]

[1]*The State Key Laboratory of Automotive Safety and Energy, Tsinghua University, Beijing 100084, People's Republic of China*
[2]*Shanxi Key Laboratory of Nano Functional Composite Materials, North University of China, Taiyuan 030051, People's Republic of China*
✉ *E-mail: weiyt@tsinghua.edu.cn*

Published in Micro & Nano Letters; Received on 7th January 2017; Revised on 1st March 2017; Accepted on 27th March 2017

Nanosheets of graphene oxide (GO) were incorporated into natural rubber (NR) to investigate the influence of the partial substitution for carbon black (CB) with GO on the crosslink structure and properties of NR composites. The results show that the dispersion of the fillers was improved by a few GO nanosheets instead of CB. The dynamic and static mechanical properties were improved by using a few GO nanosheets worth of substitution content. The NR/CB/GO (NG) composites show the lowest heat buildup value when the load of nanosheets is 1 phr, which corresponds to only 9°C. However, the comprehensive performance of the composites was poor, or even deteriorated, as the GO tended to aggregate due to the high concentrations.

1. Introduction: NR exhibits many outstanding properties, such as rolling resistance, improved wet grip, low gas permeability and high strength. Some of these properties can resemble those of synthetic rubbers [1]. Although NR exhibits outstanding performance, reinforcing fillers must be added to rubber on most occasions to obtain the proper properties needed for some applications. Reinforcement, improvements in processing and reductions in the material costs are the most important purposes, so a variety of fillers is added to rubber [2]. The enhancement of strength and strength-related properties, such as abrasion resistance, modulus and hardness, is primarily related to reinforcement [3, 4]. CB is one of the main reinforcing fillers employed in rubber industry and is useful in many applications. The tear strength, tensile strength, abrasion resistance and modulus are increased when CB is compounded with rubber. To decrease the amount of fillers, researchers use high-performance reinforcing filler, such as multiwalled carbon nanotubes [5, 6], graphene oxide (GO) and graphene [7–9], to partially replace carbon black (CB). Controllable oxidation of graphite is applied to prepare GO; in other words, abundant oxygen-containing groups are introduced into the graphene layers such that the GO is a derivative of graphene [10–12]. GO is water soluble with abundant hydrophilic groups, and stable colloidal suspensions are easily achieved [13]. Due to the excellent stability of GO aqueous suspensions, rubber/GO composites are fabricated much more conveniently by compounding GO suspensions with rubber lattices than graphene and multiwalled carbon nanotubes.

Although a number of studies have attempted to determine the mechanical performance of composites with CB and GO, the influence of CB and GO on the heat buildup and dynamic performance of vulcanisates is rarely reported. In this work, NR composites with both CB and GO were prepared to study and discuss the cure characteristics, morphological properties and mechanical properties, particularly the heat buildup and dynamic performance of the natural rubber (NR). The NR composites were obtained by using a new method that combines a modified latex co-precipitation masterbatch, by mechanical blending, and by adding GO and CB, respectively, so the composites have both high strength and good dynamic properties.

2. Experimental

2.1. Materials: The graphite powder (<48 μm) used was of industrial grade and was purchased from Qingdao East Kay Graphite Co., Ltd, China. NR (1# smoke sheet rubber) was obtained from Hainan Agricultural Reclamation Co., Ltd. The fresh NR latex (NR, 60 wt%) was supplied by the local state-owned Qionghai Lixin farm rubber processing factory. CB (N330) was purchased from China Rubber Group Carbon Black Research Institute. All other ingredients for the rubber compound were commercially available, and the ingredients were used as received.

2.2. Preparation of the nanocomposites: A modified Hummers method was used to synthesise GO via the oxidation of natural graphite powder. A Bruker GADDS X-ray diffractometer equipped with a two-dimensional area detector were used to record the X-ray diffraction (XRD) pattern using Cu-Kα radiation at a voltage of 40 kV and a current of 40 mA. A Lambda 35 Perkin Elmer spectrometer was used to record the UV–Vis spectra.

Masterbatches of GO with NR were prepared using an aqueous coagulation method. A certain amount of GO was added to 25 g of fresh NR latex, stirred for 1 h using magnetic action and coagulated by the addition of a $CaCl_2$ flocculant to produce a NR-GO masterbatch. Then, the NR-GO masterbatch was cut into small pieces and washed to remove $CaCl_2$ and dried at 70°C for at least 36 h to remove any water. A control NR sample was prepared by the same process, but with no GO added. The samples from the NR/CB/GO system vulcanisates are known as NG-*x*, where *x* refers to the mass fraction of the CB replaced by GO. The formulations of the NG composites are listed in Table 1. Other ingredients, including the NR-GO masterbatch, were mixed with NR for 15 min at 110°C in a laboratory-sized internal mixer, except for the curatives. At temperatures below 40°C, the curatives were added to the compounds using a two roll-mill. The compounds were hot-pressed and vulcanised at 150°C × T_{c90} × 13 MPa. T_{c90} was obtained using a M-3000A rheometer (High Speed Rail Instrument Testing Company, Taiwan, China).

2.3. Mechanical characterisation: According to the ISO standard 37-2005, tensile tests were performed on an AI-7000-SGD (Taiwan) instrument at 25°C. An initial clamp separation of 65 mm and a crosshead rate of 500 mm/min were used. According to the ISO standard 7619-1997, the shore A hardness was measured using an XHS-W sclerometer (Liaoning). The standard deviations for the tensile strength, modulus at 100%, 300% elongation, elongation at break, hardness and tear strength

© The Institution of Engineering and Technology 2017

Table 1 Composition of the NG nanocomposites

Samples[a]	NG-0	NG-1	NG-2	NG-3	NG-5
NR (dry)	85	85	85	85	85
NR (latex)	15	15	15	15	15
GO	0	1	2	3	5
N330	40	39	38	37	35

[a]All of the samples contain the following additives: poly(1,2-dihydro-2,2,4-trimethyl-quinoline) (1 phr), N-isopropyl-N′-phenyl-4-phenylenediamin (1 phr), zinc oxide (5 phr), stearic acid (2 phr), N-(oxidiethylene)-2-benzothiazolyl sulfenamide (2 phr) and sulphur (2 phr).

are ±0.4, ±0.1, ±0.3, ±5.0, ±1 and ±0.5 units, respectively. To study the heat ageing resistance, the samples were aged in a circulating air chamber for 22 h at 100°C. Prior to testing, the aged samples were left at room temperature at least for 18 h.

The hysteresis loss was defined as

$$H_k = (W_1 - W_2)/W_1 \times 100, \tag{1}$$

where W_1, W_2 and H_k were work performed during forward deformation, reverse deformation and hysteresis loss, respectively.

The testing samples were cut to dimensions of 90 mm × 6 mm × 2 mm, with a scale distance of 10 mm. For tensile testing, a crosshead rate of 500 mm/min was used during forward deformation and a tensile force of 1 N was used during reverse deformation. All samples were subjected to four cycles. Hysteresis testing was performed up to a tensile force of 25 N, and only the hysteresis losses for the fourth cycle were reported. The effective elasticity is defined as

$$\eta_k = W_2/W_1 \times 100. \tag{2}$$

2.4. Determination of the crosslink density: The equilibrium swelling method was used to study the crosslink density. First, to remove substances such as the remains of activators and accelerators, the samples were placed in acetone for 24 h in a soxhlet apparatus and dried in a vacuum oven at 50°C. Then, the samples were placed in toluene for 48 h at room temperature to swell prior to being weighed. Subsequently, the samples were dried to achieve a constant weight in a vacuum oven at 50°C. According to Flory–Rehner, the crosslink density was calculated [14–17] as

$$-[\ln(1 - V_r) + V_r + \chi V_r^2] = \rho v_0 M_c (V_r^{1/3} - 0.5V_r), \tag{3}$$

$$V_r = (m_2/\rho)/[m_2/\rho + (m_1 - m_2)/\rho_s], \tag{4}$$

where M_c is the crosslink density, V_r is the volume fraction of polymer in the swollen mass, ρ is the density of NR, ρ_s is the density of toluene, m_1 and m_2 are the weights of the swollen and de-swollen samples, v_0 is the molar volume of the solvent (106.2 cm^3 for toluene) and χ is the Flory–Huggins polymer–solvent interaction term, respectively.

2.5. Bound rubber: To determine the bound rubber, compounds (without curatives) were kept for 7 days at room temperature before being cut into small pieces. Samples (~0.5 g) were placed in a stainless-steel wire cage and immersed in 100 ml of toluene. On the fourth day, the solvent was renewed. The samples were removed from the solvent on the seventh day and dried in a vacuum at 60°C to a constant weight. According to the following equation, the bound rubber percentage (R_b) was determined [18]:

$$R_b(\%) = 100 \times \frac{W_{fg} - W_t[m_f/(m_f + m_r)]}{W_t}, \tag{5}$$

where m_r is the weight fraction of the polymer in the original sample, m_f is the weight fraction of the filler in the gel, W_{fg} is the weight of the dried gel and W_t is the weight of the original sample.

2.6. Filler–rubber interaction: According to the Park and Lorenz equation (6), the filler–rubber interaction was calculated using [19]

$$Q_f/Q_g = ae^{-z} + b. \tag{6}$$

where a and b are constants, z is the ratio by weight of the filler to the rubber hydrocarbons in the vulcanisates and the subscripts f and g refer to the filled and gum vulcanisates, respectively. Samples were cut into dimensions of 30 mm × 5 mm × 2 mm and then immersed in toluene for 48 h at 25°C until equilibrium swelling. The samples were dried at 60°C in an oven to a constant weight. Using (7), the toluene uptake per gram of rubber (Q) was determined

$$Q = (W_s - W_d)/(W_o \times \varphi_{rubber}) \tag{7}$$

where W_o is the original weight, W_s is the swollen weight, W_d is the dried weight and ϕ_{rubber} is the mass fraction of the rubber in the composites. Higher Q_f/Q_g values denoted fewer interactions between the filler and matrix.

2.7. Microstructure: A field emission scanning electron microscope (Hitachi S-4800, Japan) was used to measure the fractured surfaces of the composites by plating the surfaces with a thin layer of gold before observation.

2.8. Dynamic rheological properties: A rubber process analyzer (RPA) 2000 (Alpha Technologies Co., USA) was used to test the processability of the compounds. The strain amplitude varied from 0.28 to 400% and the test temperature was 60°C at 1 Hz.

2.9. Heat buildup study: A RH-3000N dynamic compression heat buildup testing instrument was used to measure the dynamic compression heat buildup based on the ISO 4666 standard. Prior to testing, the samples were preheated for 30 min at 55°C and subjected to a compressive load of 245 N at a frequency of 20 Hz with an amplitude of 4.45 mm. The increase in temperature at the base of the samples was recorded after 25 min.

2.10. Dynamic mechanical analysis: A Mettler Toledo SDTA861^e dynamic mechanical analyser was used to perform dynamic mechanical analysis. The temperature scanning range was from −100 to 100°C in tensile mode and a heating rate of 3°C min^{-1} under a liquid nitrogen flow. The test frequency was 10 Hz, and the strain was 0.5%.

3. Results and discussion

3.1. Nature of the GO: Fig. 1 shows the characteristics of the GO. From the XRD spectra of the GO sheets presented in Fig. 1*a*, we see that the characteristic sharp peak for graphite at $2\theta = 26.5°$ (shown as an inset in Fig. 1*a*) shifts to a lower angle. This phenomenon indicates the exfoliation of the individual GO sheets due to a decreased number of interlayer interactions of the functional groups. The UV–Vis spectra of the supernatants of the GO sheets are shown in Fig. 1*b*. An absorption peak centred at 228 nm and a shoulder peak at ~300 nm are assigned to the $\pi \rightarrow \pi^*$ transitions of the aromatic C–C bonds and $n \rightarrow \pi^*$ transitions of the C=O bonds, respectively [20].

3.2. Cure characteristics: Table 2 shows the cure characteristics for the compound. The torque and torque difference of the vulcanisates increase when CB is gradually replaced by GO. In these compounds, the moveability of molecular chain decreases as CB

© The Institution of Engineering and Technology 2017

doi: 10.1049/mnl.2016.0035

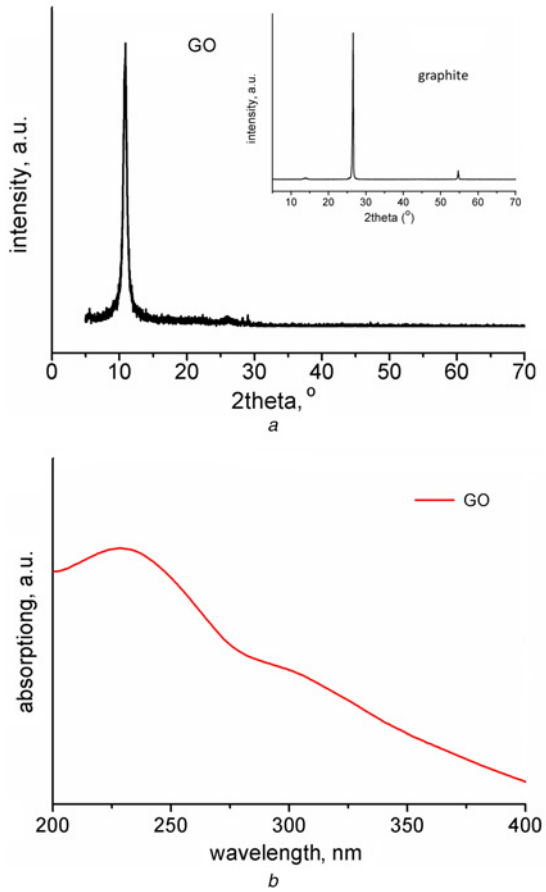

Fig. 1 *XRD and UV–Vis patterns for the GO*
a XRD patterns for the GO
b UV–Vis patterns for the GO

Table 2 Vulcanisation characteristics of the NG compounds

GO/CB ratio	T_{S2}, min	T_{c90}, min	M_H, N m	M_L, N m	$M_H - M_L$, N m	CRI, min^{-1}
0/40	2.10	4.70	2.14	0.03	2.11	38.46
1/39	2.38	4.78	2.17	0.04	2.13	41.67
2/38	2.48	4.85	2.21	0.05	2.16	42.19
3/37	2.90	6.46	2.24	0.06	2.18	28.09
5/35	2.86	6.72	2.31	0.06	2.25	25.91

is partially replaced by GO, so the torque and torque difference in the vulcanisates increase, which indicates that the reinforcement effect of the GO is greater than in the CB. Based on the difference between the optimum cure time for vulcanisation t_{c90} and the scorch time t_{s2}, the cure rate index (CRI) can be calculated using [21]

$$\mathrm{CRI} = 100/(t_{c90} - t_{s2}).$$

Both the cure time and the scorch time increase when the CB is replaced gradually by GO, which suggests the addition of GO should retard the curing. The abundant functional groups of the GO sheets tend to absorb the curing agents. Moreover, hybrid filler networks limit the diffusion of curing agents, which also retards the curing [22]. Therefore, the curing process of the NG composites is slower when significant amounts of CB are substituted by GO.

Table 3 Crosslink densities of vulcanisates ($\times 10^{-4}$ mol/cm^3)

GO/CB ratio	0/40	1/39	2/38	3/37	5/35
crosslink density	4.27	5.11	5.16	4.19	3.92
crosslink density (after ageing)	4.96	5.80	6.29	5.18	4.46

From Table 3, we see that the crosslink density of the composites initially increases with the GO and subsequently starts to decrease at a certain content of GO. The crosslink density of the NG composite is maximised when the addition of GO is 2 phr during two opposite effects. The high aspect ratio of the GO sheets may provide more physical crosslinks to the rubber. However, GO tends to absorb accelerators and then decreases crosslink density. Consequently, the vulcanisation is delayed to different degrees, but all the crosslink densities increase after ageing during post-vulcanisation.

3.3. Mechanical performance: The hardness and modulus of the NG composites are shown in Table 4. Not surprisingly, the hardness and modulus of the vulcanisates increase when the CB is substituted by GO, and the increase is marked after ageing. For equal amounts of filler, samples NG-1 and NG-2 exhibit high moduli and hardnesses, followed by the NG-3 composites. This is mainly due to the filler network structure associated with the GO being more developed and trapping more rubber, so the effective volume of the fillers increases [23, 24]. The modulus starts to decrease when the GO content is higher than 2 phr. This may be interpreted by the combination of insufficient surface adhesion resulting from the poor compatibility between the GO and NR and filler aggregation. Hence, the composites filled with higher content GO exhibit a lower modulus. After ageing, the crosslinking density, modulus and hardness of the composites increase considerably due to the post-crosslinking effect.

The tear and tensile strengths of the composites are shown in Fig. 2. When the GO content is no >2 phr, the composites exhibit

Table 4 Modulus and hardness of the aged and unaged composites

GO/CB ratio	0 / 40	1 / 39	2 / 38	3 / 37	5 / 35
100% modulus, MPa	2.80	3.50	3.46	3.26	3.10
300% modulus, MPa	14.88	15.07	15.59	13.11	12.70
hardness (shore A)	63	64	66	68	69
aged					
100% modulus, MPa	3.93	3.49	3.99	3.46	3.96
300% modulus, MPa	15.50	17.51	17.99	16.46	16.02
hardness (shore A)	67	66	68	70	72

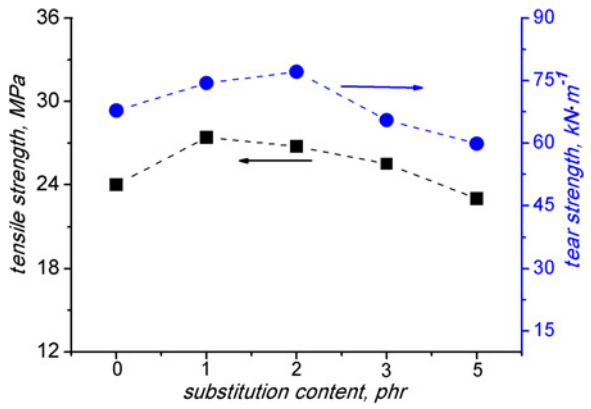

Fig. 2 *Tear and tensile strengths of all the composites*

© The Institution of Engineering and Technology 2017

increased tear and tensile strengths, which are attributed to the high reinforcing capability of the GO nanosheets. There are several factors, including stain-induced crystallisation, interfacial stress transferring, high aspect ratios, ultrastrong mechanical properties for graphene, increased crosslink density and improved dispersion of the CB, that relate to the reinforcing effects associated with graphene-based materials [25, 26]. However, when the GO nanosheet content is higher than 3 phr, the tensile strength decreases sharply due to the aggregation of the GO sheets.

Fig. 3 shows the elongation at break for all of the composites. All of the elongations at break of the GO composites are superior to those of the CB-filled composites. However, after ageing, the elongation at break of the composites decreases due to the post-crosslinking effect. The increased crosslink density of all composites can account for the reduction in the elongation at break.

3.4. Micromorphology: To analyse the significant improvement in the mechanical properties of the composites, scanning electron microscopic (SEM) images of the tensile fracture surfaces are characterised. As shown in Fig. 4, it is obvious that the GO composite surfaces (not more than 2 phr) are much rougher and contain many more protuberances than of the surfaces of the CB-filled composites due to the better dispersion, as noted above. The surfaces of the GO composites (higher than 3 phr) are smooth, which is attributed to the aggregation of the GO sheets. Moreover, the increases in the mechanical properties of GO composites are due to stronger filler–rubber interactions and the presence of more bound rubber, as shown in Table 5.

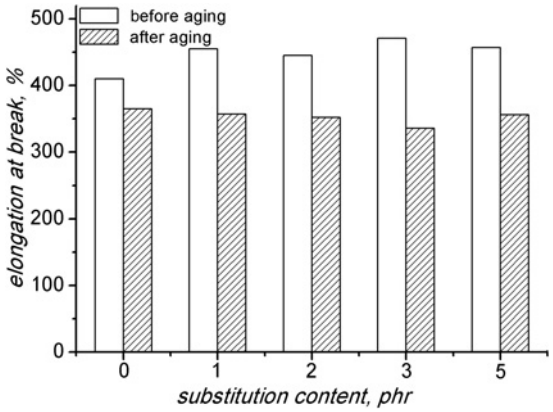

Fig. 3 *Elongation at break of all the composites*

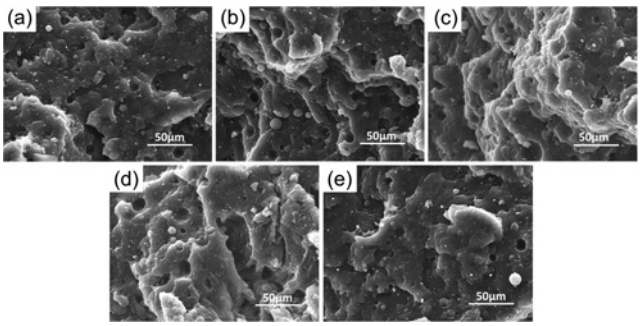

Fig. 4 *SEM images of the tensile fractured surfaces of the composites*
a NG-0
b NG-1
c NG-2
d NG-3
e NG-5

Table 5 Bound rubber content and filler–rubber interactions of the NR compounds and composites

GO/CB ratio	0/40	1/39	2/38	3/37	5/35
Rb, %	39.43	51.43	42.43	35.43	33.43
Q_f/Q_g	0.72	0.67	0.68	0.80	0.84

3.5. Heat buildup: The heat buildup of all composites is compared in Fig. 5. The results show that heat buildup decrease when CB is replaced by GO. For instance, both NG-1 and NG-2 composites show the lower heat buildup, which is due to the better dispersity and stronger filler–rubber interaction. The results suggest that the combination of latex co-precipitation masterbatch and mechanical blending method is very practical for preparing composites with a lower heat buildup.

In addition, the effective elasticity and hysteresis losses for all composites are shown in Table 6. The results show that the effective elasticity increases when the CB is partially replaced by the GO and the corresponding hysteresis losses decrease. However, the effective elasticity decreases when the concentration of GO is > 2 phr as the total amount of CB and GO is 40 phr, whereas the corresponding hysteresis loss increases due to worse dispersion.

3.6. Dynamic properties determined by RPA: The relationship between the shear strain and storage modulus of the vulcanisates is controlled by various factors, including rubber network properties, filler–rubber interaction and strong filler–filler interactions. However, at small strains, the storage modulus is mainly the result of strong filler–filler interaction.

Therefore, to study the filler network structure, the relationship between the storage modulus and shear strain is investigated in this Letter. Figs. 6*a* and *b* show the curves for G' and tanδ versus strain of the compounds, respectively. The strain dependence of the dynamic viscoelastic properties in a filled rubber compound acting as the storage modulus is known as the Payne effect [27–29]. A weaker filler network structure and a higher uniformity of the filler dispersion in the rubber matrix yield a lower Payne effect. Fig. 6*a* shows that the composites exhibit an obvious

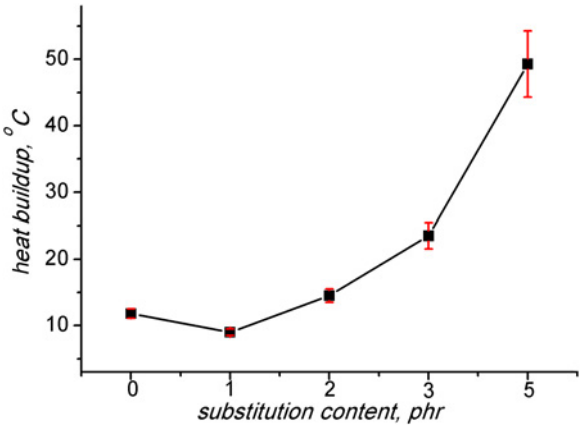

Fig. 5 *Heat buildup of all composites*

Table 6 Effective elasticity and hysteresis loss ratio for the composites

GO/CB ratio	0/40	1/39	2/38	3/37	5/35
effective elasticity, %	72.50	80.20	76.26	68.63	64.76
hysteresis loss, %	27.50	19.80	23.74	31.37	35.24

© The Institution of Engineering and Technology 2017

doi: 10.1049/mnl.2016.0035

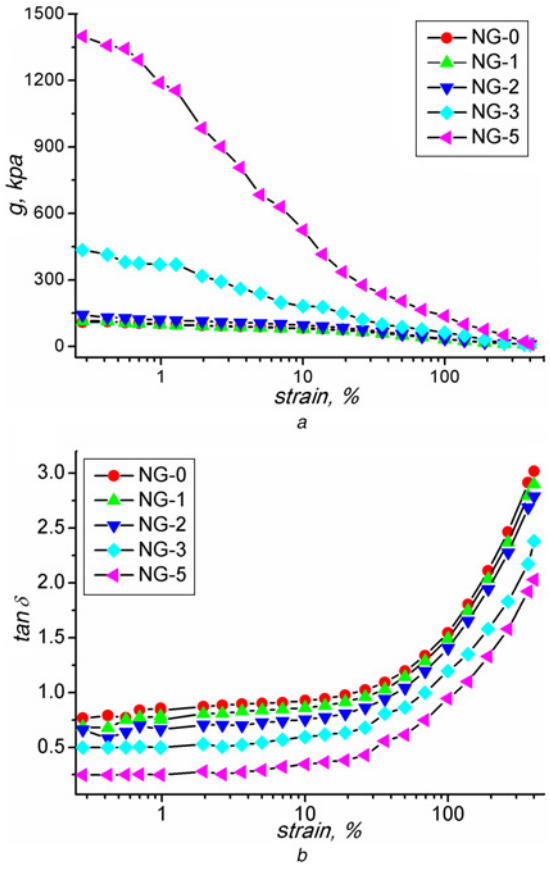

Fig. 6 *Curves of G′ and tanδ versus strain of the compounds*
a Curves of *G′* versus strain of the compounds
b Curves of tan*δ* versus strain of the compounds

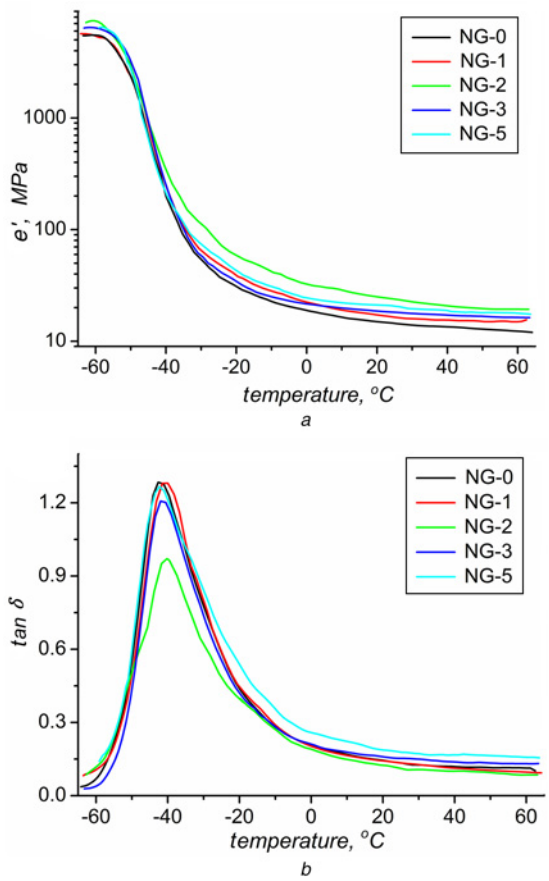

Fig. 7 *Curves of E′ and tanδ versus temperature for the vulcanisates*
a Curves of *E′* versus temperature for the vulcanisates
b Curves of tan*δ* versus temperature for the vulcanisates

Payne effect when the CB is partially replaced by GO (higher than 2 phr), particularly the NG-5 composites. In general, a rubber matrix exhibits a lower Payne effect when it is filled with a particular volume fraction of fillers, but the fillers are better dispersed. For instance, adding a silane coupling agent to a silica-filled system leads to a decrease in the Payne effect because the filler–rubber interaction develops at the expense of the filler–filler interaction [30].

Fig. 6*b* shows that when CB is partially replaced by GO, the compound exhibits a smaller tan*δ*. This is attributed to more bound rubber and the additionally hindered mobility of the rubber chains, as noted above. It is widely known that the polymer chains of filled composites are absorbed and then trapped on the surfaces of the fillers and that the flexibility and mobility of the chains are confined [31, 32]. The extent of this confinement is primarily governed by the interfacial interaction between the fillers and the polymer matrix and by the dispersion of the fillers.

3.7. Dynamic properties determined by DMA: Fig. 7 shows the dynamic mechanical spectra versus the temperature of the composites. From Fig. 7*a*, we see that compared to CB-filled composites, the modulus below the glass transition temperature for GO composites is larger. In the rubbery plateau area, the *E′* values of the GO compounds increase, and the material becomes stiffer. In fact, the strain in the samples for the dynamic mechanical analysis versus temperature is <10%. Therefore, the dynamic behaviour within this strain range is linear according to Fig. 7*a*. The filler–filler interaction mainly contributes to the storage modulus because the segmental motion is frozen in the low temperature domain. As the temperature increases to ambient and above, the filler–rubber interaction and the larger volume fraction filler dominate the storage modulus, meaning that the NG-2 composites exhibit a higher modulus than the other composites at higher temperatures.

At the glass transition temperature, the tan*δ* intensity of the GO composites decrease, as shown in Fig. 7*b*. The energy dissipation caused by internal kinetic friction of the composites can be defined by the peak value of tan*δ*, which is inversely proportional to the interfacial interaction between the fillers and the polymer matrix. The tan*δ* value of the composites (20–65°C) can be used to characterise the rolling resistance. The lower tan*δ* value for all of the NG composites facilitates a good rolling resistance. Moreover, the better dispersion and the enhancement of the stronger filler–rubber interactions result in a higher elasticity for the NG composites, which is the main reason for the lower tan*δ* value.

4. Conclusions: In this Letter, we have studied the effect that substituting GO for CB has on the structure and performance of NR/CB composites. NR/GO/CB (NG) composites exhibit better filler dispersion and dynamic properties when GO is substituted to a certain concentration compared with NR/CB composites. For instance, the sample with 1 phr GO shows the highest tensile strength, 27.41 MPa, a lower tan*δ* at 60°C and the lowest heat buildup, only 9.0°C. This is attributed not only to a large crosslink density and better filler dispersion but also to a high effective elasticity and large filler–rubber interaction. The Payne effect is not obvious when CB was partially replaced by GO (lower than 2 phr), but it clearly increased when the GO is higher than 2 phr due to the poor dispersion. At higher concentrations, GO tends to aggregate and results in poor improvements in the dynamic properties and even degrades the properties of the composites.

© The Institution of Engineering and Technology 2017

5. Acknowledgment: The National Science Foundation of China (grant no. 51275265) supported this research.

6 References

[1] Pal K., Rajasekar R., Kang D.J., *ET AL.*: 'Effect of fillers on natural rubber/high styrene rubber blends with nano silica: morphology and wear', *Mater. Des.*, 2010, **31**, p. 677

[2] Claiden P., Knowles G., Liu F., *ET AL.*: 'Modelling of nano-filler reinforcement, filler strength and experimental results of nanosilica composites made by a precipitation method', *Comput. Mater. Sci.*, 2014, **94**, p. 27

[3] Heinrich G., Kluppel M., Vilgis T.A.: 'Reinforcement of elastomers', *Curr. Opin. Solid State Mater. Sci.*, 2002, **6**, p. 195

[4] Gotz C., Lim G.T., Puskas J.E., *ET AL.*: 'The effect of carbon black reinforcement on the dynamic fatigue and creep of polyisobutylene-based biomaterials', *J. Mech. Behav. Biomed. Mater.*, 2014, **39**, p. 355

[5] Dong B., Liu C., Lu Y.L., *ET AL.*: 'Synergistic effects of carbon nanotubes and carbon black on the fracture and fatigue resistance of natural rubber composites', *J. Appl. Polym. Sci.*, 2015, **132**, p. 995

[6] Poikelisp M., Das A., Dierkes W., *ET AL.*: 'The effect of partial replacement of carbon black by carbon nanotubes on the properties of natural rubber/butadiene rubber compound', *J. Appl. Polym. Sci.*, 2013, **130**, p. 3153

[7] Yang G.W., Liao Z.F., Yang Z.J., *ET AL.*: 'Effects of substitution for carbon black with graphene oxide or graphene on the morphology and performance of natural rubber/carbon black composites', *J. Appl. Polym. Sci.*, 2015, **132**, p. 1

[8] Kim N., Kuila T., Lee J.: 'Enhanced mechanical properties of a multiwall carbon nanotube attached pre-stitched graphene oxide filled linear low density polyethylene composite', *J. Mater. Chem. A*, 2014, **8**, p. 2681

[9] Wan Y.J., Tang L.C., Gong L.X., *ET AL.*: 'Grafting of epoxy chains onto graphene oxide for epoxy composites with improved mechanical and thermal properties', *Carbon*, 2014, **69**, p. 467

[10] Hummers W.S. Jr., Offeman R.E.: 'Preparation of graphitic oxide', *J. Am. Chem. Soc.*, 1958, **80**, p. 1339

[11] Stankovich S., Piner R.D., Nguyen S.T., *ET AL.*: 'Synthesis and exfoliation of isocyanate-treated graphene oxide nanoplatelets', *Carbon*, 2006, **44**, p. 3342

[12] Dreyer D.R., Park S., Bielawski C.W., *ET AL.*: 'The chemistry of graphene oxide', *Chem. Soc. Rev.*, 2010, **39**, p. 228

[13] Stankovich S., Dikin D.A., Piner R.D., *ET AL.*: 'Synthesis of graphene-based nanosheets via chemical reduction of exfoliated graphite oxide', *Carbon*, 2007, **45**, p. 1558

[14] Xu C.H., Chen Y.K., Wang Y.P., *ET AL.*: 'Temperature dependence of the mechanical properties and the inner structures of natural rubber reinforced by in situ polymerization of zinc dimethacrylate', *J. Appl. Polym. Sci.*, 2013, **128**, p. 2350

[15] Singh A.: 'Synthesis and applications of polyacrylamide gels catalyzed by silver nitrate', *J. Appl. Polym. Sci.*, 2011, **119**, p. 1084

[16] Sirousazar M., Kokabi M., Hassan Z.M.: 'Swelling behavior and structural characteristics of polyvinyl alcohol/montmorillonite nanocomposite hydrogels', *J. Appl. Polym. Sci.*, 2012, **123**, p. 50

[17] Mao Y.Y., Wen S.P., Chen Y.L., *ET AL.*: 'High performance graphene oxide based rubber composites', *Sci. Rep.-UK*, 2013, **3**, p. 1

[18] Qu L.L., Yu G.Z., Wang L.L., *ET AL.*: 'Effect of filler–elastomer interactions on the mechanical and nonlinear viscoelastic behaviors of chemically modified silica-reinforced solution-polymerized styrene butadiene rubber', *J. Appl. Polym. Sci.*, 2012, **126**, p. 116

[19] Lorenz O., Parks C.R.: 'The crosslinking efficiency of some vulcanizing agents in natural rubber', *J. Polym. Sci.*, 1961, **50**, p. 299

[20] Li D., Muller M.B., Gilje S., *ET AL.*: 'Processable aqueous dispersions of graphene nanosheets', *Nat. Nanotechnol.*, 2008, **3**, p. 101

[21] Darwish N.A., Shehata A.B., Abd El-Megeed A.A., *ET AL.*: 'Compatibilization of SBR/NBR blends using poly acrylonitrile as compatibilizer', *Polym. Plast. Technol. Eng.*, 2005, **44**, p. 1297

[22] Sepehri A., Razzaghi-Kashani M., Ghoreishy M.: 'Vulcanization kinetics of butyl rubber–clay nanocomposites and its dependence on clay microstructure', *J. Appl. Polym. Sci.*, 2012, **125**, p. 204

[23] Wang M.J.: 'Effect of polymer-filler and filler–filler interactions on dynamic properties of filled vulcanizates', *Rubber Chem. Technol.*, 1998, **71**, p. 520

[24] Liu Y.B., Li L., Wang Q.: 'Effect of carbon black/nanoclay hybrid filler on the dynamic properties of natural rubber vulcanizates', *J. Appl. Polym. Sci.*, 2010, **118**, p. 1111

[25] Li F.Y., Yan N., Zhan Y.H., *ET AL.*: 'Probing the reinforcing mechanism of graphene and graphene oxide in natural rubber', *J. Appl. Polym. Sci.*, 2013, **129**, p. 2342

[26] Zhan Y., Wu J., Xia H., *ET AL.*: 'Dispersion and exfoliation of graphene in rubber by an ultrasonically-assisted latex mixing and in situ reduction process', *Macromol. Mater. Eng.*, 2011, **296**, p. 590

[27] Sorokin V.V., Ecker E., Stepanov V.G., *ET AL.*: 'Experimental study of the magnetic field enhanced Payne effect in magnetorheological elastomers', *Soft Matter*, 2014, **10**, p. 8765

[28] Luginsland H.D., Frohlich J., Wehmeier A.: 'Influence of different silanes on the reinforcement of silica-filled rubber compounds', *Rubber Chem. Technol.*, 2002, **75**, p. 563

[29] Li Y., Han B.Y., Wen S.P., *ET AL.*: 'Effect of the temperature on surface modification of silica and properties of modified silica filled rubber composites', *Compos. A*, 2014, **62**, p. 52

[30] Reuvekamp L.A.E.M., ten Brinke J.W., van Swaaij P.J., *ET AL.*: 'Effects of time and temperature on the reaction of TESPT silane coupling agent during mixing with silica filler and tire rubber', *Rubber Chem. Technol.*, 2002, **75**, p. 187

[31] Wu S.W., Tang Z.H., Guo B.C., *ET AL.*: 'Effects of interfacial interaction on chain dynamics of rubber/graphene oxide hybrids: a dielectric relaxation spectroscopy study', *RSC Adv.*, 2013, **3**, p. 14549

[32] Liu J., Wu Y., Shen J.X., *ET AL.*: 'Polymer-nanoparticle interfacial behavior revisited: a molecular dynamics study', *Phys. Chem. Chem. Phys.*, 2011, **13**, p. 13058

© The Institution of Engineering and Technology 2017

doi: 10.1049/mnl.2016.0035